Inorg. Chem. **2005**, *44*, 5654–5660

Extending the Nitrogen-Heterosuperbenzene Family: The Spectroscopic, Redox, and Photophysical Properties of "Half-Cyclized" N-$^1/_2$HSB and Its Ru(II) Complex

Daniel J. Gregg,[†] Eberhard Bothe,[‡] Petra Höfer,[‡] Paolo Passaniti,[§] and Sylvia M. Draper*[,†]

Department of Chemistry, University of Dublin, Trinity College, D2, Ireland, Max-Plank Institute Für Bioanorganische Chemie, 34-36 Stiftstrasse, 45470 Muelheim, Germany, and Dipartimento di Chimica "G. Ciamician", Università di Bologna, 40126 Bologna, Italy

Received March 4, 2005

Oxidative cyclodehydrogenation is an important process in the formation of the new graphene, N-$^1/_2$HSB **2**. This heteropolyaromatic results from the $FeCl_3$-catalyzed oxidative cyclodehydrogenation of 1,2-dipyrimidyl-3,4,5,6-tetra-(4-*tert*-butylphenyl)benzene. Three new C–C bonds are formed that lock the two pyrimidines in a molecular platform comprising eight fused aromatic rings flanked by two remaining "uncyclized" phenyl rings. Mechanistically intriguing is the fact that N-HSB **1**, the product of six C–C bond fusions, is co-synthesized with its "half-cyclized" daughter in this reaction. **1** and **2** have the same bidentate N-atom arrangement. This facilitates formation of the heteroleptic Ru(II) complexes, $[Ru(bpy)_2(\mathbf{2})](PF_6)_2$ **4** and $[Ru(bpy)_2(\mathbf{1})](PF_6)_2$ **3**, which differ in the size and planarity of their aromatic ligands. The new ligand **2** and its complex **4** are characterized by ^{1}H NMR, IR, ESI-MS, and accurate mass methods. **2** exhibits photophysical properties that are consistent with a reduction of the π/π^* framework, a concomitant increase in the energy of the LUMO, and a blue-shift of the solvent-dependent fluorescence (λ_{em} = 474 nm, ϕ_F = 0.55, toluene) as compared to its parent. Complex **4** absorbs throughout the visible region and borders on near-IR emitter character, exhibiting a slightly blue-shifted ^{3}MLCT emission (868 nm, CH_3CN) as compared to that of $[Ru(bpy)_2(\mathbf{1})](PF_6)_2$ **3** (880 nm, CH_3CN). Electrochemical analyses permit further elucidation of the intermolecular interactions of **3** and **4**. These and the concentration and temperature-dependent NMR spectra of **4** confirm it to be nonaggregating, a direct result of the two uncyclized and rotatable phenyl rings in **2**.

Introduction

Our recent work heralded the arrival of the founding member of a new family of planar aromatic compounds: the nitrogen-heterosuperbenzenes.[1] Synthesized via the oxidative cyclodehydrogenation of its oligophenylene precursor, N-HSB **1** was shown to exhibit some remarkable properties both in its own right and as a ligand.[2] Among these are superior electron-acceptor characteristics as compared to its all-carbon analogue and significant electron delocalization. Such properties, which make it a promising material for application in optoelectronics, are partly the result of the presence of four outer imine N atoms. Being of pyrimidyl origin, these N atoms are strategically positioned for bidentate coordination to transition metal complexes. Most notably, the exceptionally low-lying π^* of **1** confers on its Ru(II) complex the properties of both "black" MLCT (metal-to-ligand charge-transfer) absorber and near-IR-emitter.[3]

Molecular aromatic platforms such as those offered by N-HSB **1** and now N-$^1/_2$HSB **2** are rare, eilatin being an

* To whom correspondence should be addressed. E-mail: smdraper@tcd.ie.
† Trinity College.
‡ Max-Plank Institute Für Bioanorganische Chemie.
§ Università di Bologna.

(1) Draper, S. M.; Gregg, D. J.; Madathil, R. *J. Am. Chem. Soc.* **2002**, *124*, 3486−3487.
(2) Draper, S. M.; Gregg, D. J.; Schofield, E. R.; Browne, W. R.; Duati, M.; Vos, J. G.; Passaniti, P. *J. Am. Chem. Soc.* **2004**, *126*, 8694−8701.
(3) (a) Treadway, J. A.; Strouse, G. F.; Ruminski, R. R.; Meyer, T. J. *Inorg. Chem.* **2001**, *40*, 4508−4509. (b) Chiorboli, C.; Bignozzi, C. A.; Scandola, F.; Ishow, E.; Gourdon, A.; Launay, J.-P. *Inorg. Chem.* **1999**, *38*, 2402−2410. (c) Nazeeruddin, M. K.; Péchy, P.; Grätzel, M. *Chem. Commun.* **1997**, 1705−1706. (d) Anderson, P. A.; Strouse, G. F.; Treadway, J. A.; Keene, F. R.; Meyer, T. J. *Inorg. Chem.* **1994**, *33*, 3863−3864 and references within. (e) Treadway, J. A.; Loeb, B.; Lopez, R.; Anderson, P. A.; Keene, F. R.; Meyer, T. J. *Inorg. Chem.* **1996**, *35*, 2242−2246. (f) Anderson, P. A.; Keene, F. R.; Meyer, T. J.; Moss, J. A.; Strouse, G. F.; Treadway, J. A. *J. Chem. Soc., Dalton Trans.* **2002**, 3820−3831. (g) Shen, Y.; Maliwal, B. P.; Lakowicz, J. R. *J. Fluoresc.* **2003**, *13*, 163−168.

10.1021/ic050335n CCC: $30.25
Published on Web 07/13/2005

alternative natural example.[4,5] As a result, the polyimine ligand frameworks available to the coordination chemist are relatively restricted,[6] a limitation that is significant in the search for new materials based on the tuning of the desirable photophysical properties of Ru(II) polypyridyl centers. Here, "large-surface" ligands have an important role to play in modifying the lowest energy ^{1}MLCT absorption and ^{3}MLCT-based luminescence bands of heteroleptic Ru(II) polypyridyl complexes. The recent observation of fully reversible voltage dependent color-switching by polymer embedded Ru(II) polypyridyl complexes is just one example where the electron-accepting and delocalized nature of the ligands can have a profound effect on potential applications.[7]

We are now in a position to report the formation of a next-generation nitrogen-heterosuperbenzene, the daughter "half-cyclized" N-$^1/_2$HSB **2**, and to detail the spectroscopic, redox, and photophysical properties of it and its Ru(II) complex, $[Ru(bpy)_2(\mathbf{2})](PF_6)_2$ **4** (where bpy = 2,2′-bipyridine).

Experimental Section

$RuCl_3 \cdot H_2O$ (Johnson-Matthey) and 2,2′-bipyridine (bpy) (Aldrich) were used as received. $[Ru(bpy)_2Cl_2] \cdot 2H_2O$[8] and 1,2-dipyrimidyl-3,4,5,6-tetra-(4-*tert*-butylphenyl)benzene[1] were synthesized according to literature procedures. All reactions were carried out under an argon atmosphere using standard schlenck techniques. Flash chromatography was performed using silica gel (Brockman I, Aldrich Chemical) as the stationary phase. Preparative thin-layer chromatography was performed using silica gel (1000 μm thickness) preparative thin layer chromatographic plates (Aldrich).

Synthesis of Half-Cyclized N-$^1/_2$HSB (2). A solution of iron(III)chloride (0.425 g, 2.62 mmol) in nitromethane (3 mL) was added dropwise to a stirred solution of 1,2-dipyrimidyl-3,4,5,6-tetra-(4-*tert*-butylphenyl)benzene (100 mg, 0.131 mmol) in dichloromethane (30 mL). An argon stream was bubbled through the reaction mixture throughout the entire reaction. After being stirred for another 30 min, the reaction was quenched with methanol (20 mL). The product was extracted into chloroform, washed with water, and dried over $MgSO_4$. Following preparative thin-layer chromatography (SiO_2, 1:9 methanol:toluene), **2** was recrystallized from dichloromethane/diethyl ether to give a yellow crystalline solid (32 mg, 32%), mp > 300 °C. ^{1}H NMR ($C_2D_2Cl_4$): δ 10.11 (s, 2H, H1), 9.62 (s, 2H, H2), 7.83 (d, 2H, $^3J_{HH}$ = 9.8, H4), 7.37 (d, 2H, $^3J_{HH}$ = 8.8, H3), 7.25 (d, 4H, $^3J_{HH}$ = 7.8, H6), 7.02 (d, 4H, $^3J_{HH}$ = 7.8, H5), 1.46 (s, 18H, $-CH_3$), 1.32 (s, 18H, $-CH_3$). ^{1}H NMR ($CDCl_3$): δ 10.14 (s, 2H, H1), 9.65 (d, 2H, $^4J_{HH}$ = 2.1, H2), 7.82 (d, 2H, $^3J_{HH}$ = 9.6, H4), 7.39 (dd, 2H, $^3J_{HH}$ = 9.6, $^4J_{HH}$ = 2.1, H3), 7.25 (d, overlapped with solvent peak, H6), 7.05 (d, 4H, $^3J_{HH}$ = 8.2, H5), 1.51 (s, 18H, $-CH_3$), 1.36 (s, 18H, $-CH_3$). ES-MS ($CHCl_3$) *m*/*z* (%) $(MH)^+$ 757.2 (100) (calcd 758.0); ESI-MS ($CHCl_3$) calculated for $C_{54}H_{53}N_4$, $(MH)^+$ *m*/*z* 757.4270; found, 757.4282. IR (KBr disk, cm^{-1}): 3040m, 2963vs, 2868m, 1639m, 1562s, 1530s, 1513s, 1462m, 1361s, 1260s, 1119m, 1025m, 843s, 791m, 683m, 558m.

Synthesis of $[Ru(bpy)_2(2)](PF_6)_2$ (4). Compound **2** (100 mg; 0.13 mmol) and $[Ru(bpy)_2Cl_2] \cdot 2H_2O$ (76 mg; 0.16 mmol) were sonicated in diethylene glycol ethyl ether (15 mL) for 10 min. The brown solution was degassed by passing a stream of argon through the solution for 30 min. After the solution was heated for 20 h at 127 °C under an argon atmosphere, it was allowed to cool to room temperature and was filtered. To the mixture was added a saturated NH_4PF_6 aqueous solution to form a dark green solid, which was separated by filtration and washed with water and diethyl ether. Chromatography (SiO_2, 100:10:1 acetonitrile:water:KNO_3 (aq)) followed by anion exchange gave $[Ru(bpy)_2(\mathbf{2})](PF_6)_2$ as a black-green solid. Yield: 85 mg, 36%. ^{1}H NMR (CD_3CN): δ 9.51 (d, 2H, $^4J_{HH}$ = 2.0, H2), δ 9.16 (s, 2H, H1), 8.64 (d, 2H, $^3J_{HH}$ = 8.0, H3b), 8.56 (d, 2H, $^3J_{HH}$ = 8.0, H3b′), 8.22 (t, 2H, $^3J_{HH}$ = 8.0, H4b), 8.02 (m, 4H, H4b′, H6b), 7.90 (d, 2H, $^3J_{HH}$ = 9.5, H4), 7.85 (d, 2H, $^3J_{HH}$ = 5.5, H6b′), 7.58 (m, 4H, H5b, H3), 7.39 (d, 4H, $^3J_{HH}$ = 8.5, H6), 7.18 (m, 6H, H5b′, H5), 1.43 (s, 18H, $-CH_3$), 1.37 (s, 18H, $-CH_3$). ESI-MS (CH_3CN) *m*/*z* (%) $[M - 2PF_6]^{2+}$ 585.2 (100) (calcd 585.2); ESI-MS (CH_3CN) calculated for $C_{74}H_{68}N_8Ru$, $[M - 2PF_6]^{2+}$ *m*/*z* 585.2289; found, 585.2305. IR (KBr disk, cm^{-1}): 2961s, 2910s, 2881s, 1615m, 1557s, 1465m, 1363m, 1260s, 1161m, 1103m, 843vs, 768m, 558s.

Physical Measurements and Instrumentation. IR spectra were recorded from KBr disks on a Perkin-Elmer Paragon 1000 Fourier transform spectrophotometer. NMR spectra were recorded on DPX 400 spectrometer operating at 400.13 MHz for ^{1}H and were standardized with respect to TMS. Electrospray mass spectra were recorded on a micromass LCT electrospray mass spectrometer. Accurate mass spectra were referenced against Leucine Enkephalin (555.6 g mol^{-1}) and were reported within 5 ppm.

UV−vis absorption spectra were recorded on a Shimadzu UV-2401PC, UV−vis recording spectrophotometer. The emission spectra for **2** were not corrected and were recorded at 25 °C using a Perkin-Elmer LS508B luminescence spectrometer, equipped with a Hamamatsu R928 red sensitive detector. The NIR luminescence spectra for **4** were obtained with an Edinburgh FLS920 spectrometer equipped with a Hamamatsu R5509-72 supercooled photomultiplier tube (193 K) and a TM300 emission monochromator with NIR grating blazed at 1000 nm; a 450 W xenon arc lamp was used as light source. The emission spectra were corrected to compensate for the photomultiplier response in the different spectral regions. Quartz cells (10 mm path length) were used. Emission quantum yields were measured at room temperature in air-equilibrated solutions using $[Ru(bpy)_2(\mathbf{1})](PF_6)_2$ **3** as reference compound.[2] Confirmation that O_2 concentration played no part in the luminescence measurements was obtained by reproducing the experiments in degassed solvents. Luminescence lifetime measurements were obtained using an Edinburgh Analytical Instruments (EAI) time-correlated single-photon counting apparatus (TCSPC), equipped with a Hamamatsu R928-P photomultiplier tube (ca. −20 °C); the excitation impulse was obtained by a pulsed diode laser (640 nm Picoquant; repetition frequency: 5.0 MHz). Data correlation and manipulation were carried out using EAI F900 software version 6.35. Emission lifetimes were calculated using a single-exponential fitting function; a Levenberg−Marquardt algorithm with iterative reconvolution Edinburgh instruments F900 software was used; uncertainty was ±10%. The reduced χ^2 and residual plots were used to judge the quality of the fits.

(4) Gut, D.; Goldberg, I.; Kol, M. *Inorg. Chem.* **2003**, *42*, 3483−3491.
(5) (a) Bergman, S. D.; Reshef, D.; Groysman, S.; Goldberg, I.; Kol, M. *Chem. Commun.* **2002**, 2374−2375. (b) Bergman, S. D.; Goldberg, I.; Barbieri, A.; Barigelletti, F.; Kol, M. *Inorg. Chem.* **2004**, *43*, 2355−2367. (c) Gut, D.; Rudi, A.; Kopilov, J.; Goldberg, I.; Kol, M. *J. Am. Chem. Soc.* **2002**, *124*, 5449−5456. (d) Rudi, A.; Kashman, Y.; Gut, D.; Lellouche, F.; Kol, M. *Chem. Commun.* **1997**, 17−18. (e) Bergman, S. D.; Reshef, D.; Frish, L.; Cohen, Y.; Goldberg, I.; Kol, M. *Inorg. Chem.* **2004**, *43*, 3792−3794.
(6) Glazer, E. C.; Tor, Y. *Angew. Chem., Int. Ed.* **2002**, *41*, 4022−4026.
(7) (a) Slinker, J.; Bernards, D.; Houston, P. L.; Abruña, H. D.; Bernhard, S.; Malliaras, G. G. *Chem. Commun.* **2003**, 2392−2399. (b) Welter, S.; Brunner, K.; Hofstraat, J. W.; De Cola, L. *Nature* **2003**, *421*, 54−57.
(8) Sullivan, B. P.; Salmon, D. J.; Meyer, T. J. *Inorg. Chem.* **1978**, *17*, 3334−3341.

Electrochemical voltammetric measurements (cyclic voltammetry, CV, and square-wave voltammetry, SQW) were performed on EG&G equipment (potentiostat/galvanostat model 273A) at ambient temperature. Typical concentrations were 1 mM in anhydrous solutions containing 0.1 M tetrabutylammonium hexafluorophosphate ($(n\text{-Bu})_4NPF_6$) as supporting electrolyte. Conventional voltammetric measurements were carried out using a standard three-electrode cell arrangement. A Teflon shrouded glassy carbon working electrode, a Pt wire auxiliary electrode, and a Ag/Ag^+ (0.01 M $AgNO_3$) reference electrode were employed. Solutions were deoxygenated by purging with Ar gas for 15 min prior to the measurement. Small amounts of ferrocene were added as an internal standard after completion of a set of experiments, and potentials are referenced versus the ferrocenium/ferrocene (Fc^+/Fc) couple. Controlled potential coulometry (CPC) experiments were carried out in a quartz glass electrolysis vessel consisting of an optical cuvette ($d = 0.5$ cm) mounted in the cell holder of the spectrophotometer (Hewlett-Packard HP 8543). 8 mL solutions (0.12 mM) were electrolyzed at a Pt net working electrode. Stirring was maintained with a stream of Ar gas. The counter electrode (Pt brush) and working electrode compartments were separated by a Vycor fritte.

X-band EPR spectra were recorded on a Bruker ESP 300E spectrometer equipped with a helium flow cryostat (Oxford Instruments ESR 910), an NMR field probe (Bruker 035M), and a microwave frequency counter (HP5352B).

Results and Discussion

The co-synthesis of red/brown N-HSB **1** (35% yield) and its yellow "half-cyclized" daughter **2** (32% yield) from 1,2-dipyrimidyl-3,4,5,6-tetra-(4-*tert*-butylphenyl)benzene is remarkable and unique to a synthetic regime employing $FeCl_3$[9] as oxidative cyclodehydrogenation catalyst (Scheme 1). The formation of **2** was not observed when $AlCl_3/CuCl_2$ was used in the synthesis of **1** from the same dipyrimidyl precursor. Evidently, the change of oxidative cyclodehydrogenation catalyst has a dramatic effect on the progress of the reaction such that the formation of both **1** and **2** is possible, where **1** is the result of all six and **2** is the result of one-half of the possible C−C ring fusions taking place.

The fusion of the pyrimidyl rings in both **1** and **2** suggests that the ortho hydrogen atoms of these rings are activated over their phenyl equivalents. At first glance, it seems reasonable to propose that **2** might be a precursor in the formation of **1** in the presence of $FeCl_3$, **2** being formed by an incomplete but stepwise cyclic C−C bond formation process similar to that proposed for hexa-*peri*-benzocoronenes.[10] However, **2** does not undergo further C−C ring fusion either on extended reaction in the presence of $FeCl_3$ or under forcing conditions in the presence of $AlCl_3/CuCl_2$. It seems that **2** is a thermodynamically stable product in its own right generated in a process that may be unconnected to that of its parent.

Scheme 1. N-HSB Ligand **1**, N-$^1/_2$HSB Ligand **2**, and the Synthetic Route for Generating $[Ru(bpy)_2(\mathbf{1})]^{2+}$ **3** and $[Ru(bpy)_2(\mathbf{2})]^{2+}$ **4**[a]

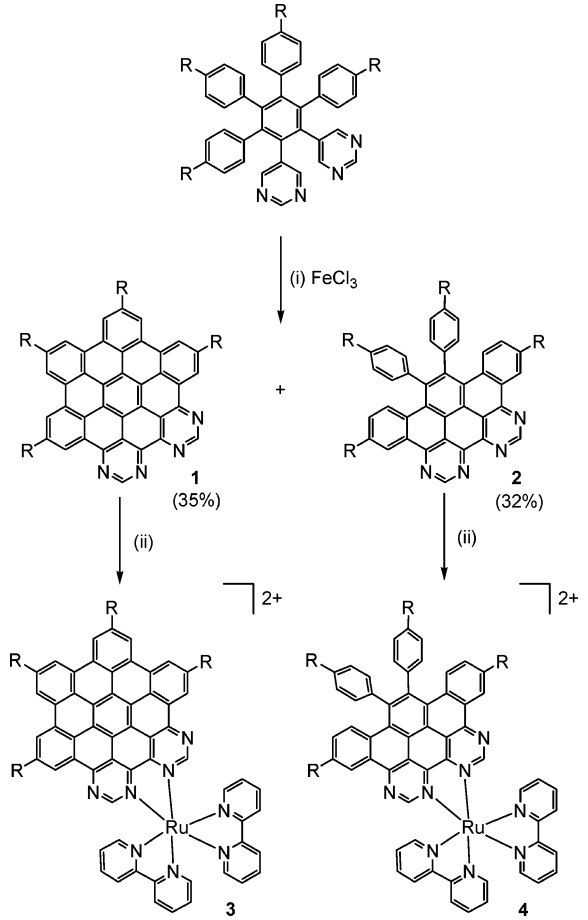

[a] Reaction conditions: (i) ref 9; (ii) $[Ru(bpy)_2Cl_2]$, 400 K, 20 h, diethylene glycol ethyl ether. R = *tert*-butyl.

Clearly, the factors affecting the cyclodehydrogenation step are complex, but the nature and sensitivity of the catalyst seem key to the possibility of controlling its outcome. **2**, by virtue of the same fused pyrimidyl ring-arrangement as its parent, provides a model compound for comparison with **1** and for investigating the influence of a reduced aromatic platform on the electrochemical and photophysical properties of nitrogen-heterosuperbenzenes generally.

The formation of **1** was verified spectroscopically by comparison to earlier work.[1] **2** is comprised of eight fused aromatic rings, unlike the 13 of its "parent", and two "uncyclized" phenyl rings, which can rotate out-of-the-plane defined by its reduced aromatic platform. Nevertheless, it retains a C_2 symmetry axis, which simplifies its ^1H NMR spectrum. The result is the appearance of just two aliphatic signals for the two sets of equivalent *tert*-butyl protons (δ 1.32 *tert*-butyls of "uncyclized" and δ 1.46 *tert*-butyls of cyclized phenyl rings, respectively). These integrate for 18 hydrogens each, leaving six aromatic signals that collectively integrate for 16 hydrogen atoms. It is the integration, coupling patterns, and chemical shifts of these aromatic signals that confirm that the three C−C bond fusions have occurred chemoselectivity at the pyrimidine-end of the molecule. The lowest field signal in the spectrum (δ 10.11) is attributed to the two aromatic hydrogen atoms situated

(9) (a) Ito, S.; Wehmeier, M.; Brand, J. D.; Kübel, C.; Epsch, R.; Rabe, P. J.; Müllen, K. *Chem.-Eur. J.* **2000**, *6*, 4327−4342. (b) Iyer, V. S.; Wehmeier, M.; Brand, J. D.; Keegstra, M. A.; Müllen, K. *Angew. Chem., Int. Ed. Engl.* **1997**, *36*, 1604−1607.

(10) (a) Rempala, P.; Kroulssk, J.; King, B. J. *J. Am. Chem. Soc.* **2004**, *126*, 15002−15003. (b) Kübel, C.; Eckhardt, K.; Enkelmann, V.; Wegner, G.; Müllen, K. *J. Mater. Chem.* **2000**, *10*, 879−886.

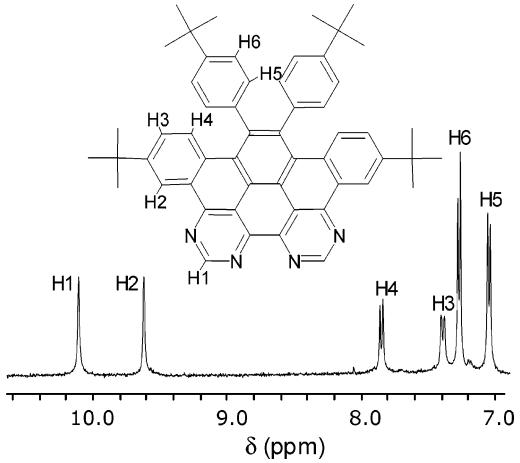

Figure 1. The aromatic region of the ^{1}H NMR spectrum of N-$^1/_2$HSB **2** ($C_2D_2Cl_4$, 21 °C, 400 MHz). The inset shows the atom labeling scheme for **2**.

between the imine nitrogen atoms (H1). Signals at δ 9.62, δ 7.83, and δ 7.37 each integrate for two hydrogen atoms and were assigned to H2, H4, and H3, respectively (for atom labeling, see Figure 1). The two phenyl rings that remain "uncyclized" appear as two doublets at δ 7.25 for H6 and δ 7.02 for H5, each integrating for four hydrogen atoms. The aromatic assignments could be made using well-resolved coupling information from ^{1}H NMR and ^{1}H−^{1}H TOCSY NMR spectra and nOe experiments.

As was observed for **1**,[1] the high thermal stability of the fused core of **2** prevented useful elemental analysis.[9b,11] However, the accurate mass ESI-spectrum of **2** showed a single isotopic envelope at *m*/*z* 757.4282 assigned to $(C_{54}H_{53}N_4)^+$ and in accord with the calculated value.

The green Ru(II) complex $[Ru(bpy)_2(\mathbf{2})]^{2+}$ **4** was prepared in a 36% yield from the reaction of *cis*-$[Ru(bpy)_2Cl_2]$ and **2** via a method analogous to that developed for **3**.[2] Complex **4** was characterized by ^{1}H NMR spectroscopy, ESI-MS, and accurate mass spectrometry. The ESI-accurate mass spectrum of **4** showed a single isotopic envelope at *m*/*z* 585.2305, assigned to $[M - 2PF_6]^{2+}$ with peaks in the envelope at $^1/_2$ mu intervals.

In the ^{1}H NMR spectra of **4**, two aliphatic signals are observed at δ 1.43 (18H) and δ 1.37 (18H) due to the resonance of the *tert*-butyl protons of coordinated **2**. The six aromatic signals of protons H1−6 of coordinated **2** (see Figure 1 for atom labeling scheme of coordinated **2**) were assigned from their coupling patterns and ^{1}H−^{1}H TOCSY spectra. The signal for the H1 protons appears significantly upfield in **4** as compared to those of the free ligand ($CDCl_3$: δ 9.06 in the complex, δ 10.14 in the free ligand). This shift is consistent with these protons pointing toward the shielding face of a pyridine ring on an adjacent bpy ligand. The aromatic protons H2−H6 resonate at δ 9.51, δ 7.58, δ 7.90, δ 7.18, and δ 7.39, respectively (see Figure 2).

Assignment of the chemical shifts for the aromatic protons of the two bpy ligands of **4** (see Figure 2 for atom labeling of pyridyl protons) has been made from their coupling

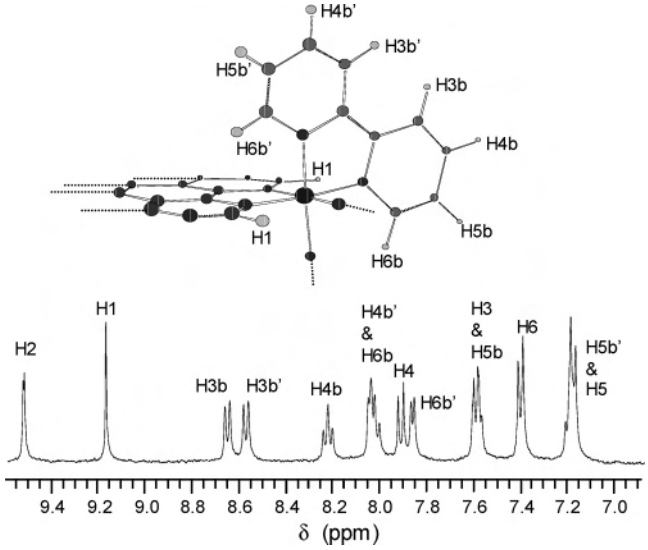

Figure 2. The atom labeling scheme for the bipyridyl protons of **4** and the aromatic region of the ^{1}H NMR spectrum of **4** (CD_3CN, 21 °C, 400 MHz).

patterns, ^{1}H−^{1}H TOCSY spectra, and by comparison with data reported for similar complexes such as $[Ru(bpy)_2(phen)]^{2+}$ (where phen = 1,10-phenanthroline)[12] and $[Ru(bpy)_2(\mathbf{1})](PF_6)_2$ **3**.[2] The four signals at δ 8.56, δ 8.02, δ 7.18, and δ 7.85 in CD_3CN are assigned to the protons H3b′, H4b′, H5b′, and H6b′, respectively, and resonate upfield of H3b, H4b, H5b, and H6b (δ 8.64, δ 8.22, δ 7.58, and δ 8.02). This is a result of the influence of the ring current of the large, rigid, aromatic section of **2** on the H3b′, H4b′, H5b′, and H6b′ protons and was similarly reported for **3**.

Whereas **3** showed dimeric aggregation in solution, **4** exhibits no concentration or temperature dependence in its ^{1}H NMR spectra. This is a result of the reduced aromatic framework of **2** and the nonplanarity of the "unfused" benzene rings, which are expected to be twisted out-of-the-plane for steric reasons.

Electrochemical Properties. Cyclic and square wave voltammograms (CV and SQW) of compounds **1**−**4** have been recorded in CH_2Cl_2 (for **1** and **2**) or CH_3CN (for **3** and **4**) solutions. The redox potentials of **1**−**4**, obtained from the voltammograms, are presented in Table 1.

Despite considerable differences in the size of their conjugated surface, the cyclic voltammograms of **1** and **2** in dichloromethane exhibit two reversible reductions at very similar redox potentials (see Table 1). The higher conjugated surface of **1** is facilitating electron acception into the aromatic system, but only by a small amount (0.03−0.04 V). The second reduction processes for both **1** and **2** (around −2.0 V) display broadened peaks with scan rate-dependent peak separation typical of a chemically reversible redox process with somewhat sluggish heterogeneous electron-transfer kinetics. There is a third irreversible reduction process detectable only as a peak in the square wave voltammogram for N-HSB **1** at −2.32 V.

(11) Simpson, C. D.; Brand, J. D.; Berresheim, A. J.; Przybilla, L.; Räder, H. J.; Müllen, K. *Chem.—Eur. J.* **2002**, *8*, 1424−1429.

(12) (a) Ye, B. H.; Chen, X. M.; Zeng, T. X.; Ji, L. N. *Inorg. Chim. Acta* **1995**, *240*, 5−11. (b) Hua, X.; von Zelewsky, A. *Inorg. Chem.* **1995**, *34*, 5791−5797. (c) Wu, F.; Riesgo, E.; Pavalova, A.; Kipp, R. A.; Schmehl, R. H.; Thummel, R. P. *Inorg. Chem.* **1999**, *38*, 5620−5628.

Table 1. Formal Electrode Potentials for Compounds **1**−**4**[a]

	oxidation (V vs Fc^+/Fc) (ΔEp (mV))		reduction (V vs Fc^+/Fc) (ΔEp (mV))			
compound	ligand	Ru^{III}/Ru^{II}	ligand reduction processes			
1	0.90[b]		−1.56 (60)	−2.00 (102)	−2.32[b]	
2			−1.59 (68)	−2.04 (142)		
3	1.26 (150)	0.95 (72)	−0.93[c] (112)	−1.43 (64)	−1.98 (68)	−2.24 (74)
4		0.95 (75)	−0.95 (69)	−1.47 (72)	−1.99 (78)	−2.26 (81)

[a] Redox potentials are given in dichloromethane (**1** and **2**) or acetonitrile (**3** and **4**) and referenced vs the ferrocinium/ferrocene-couple using Ag/Ag^+ reference electrode with 0.1 M Bu_4NPF_6 as supporting electrolyte. [b] Redox process is irreversible.[13] [c] This SQW peak is broadened.

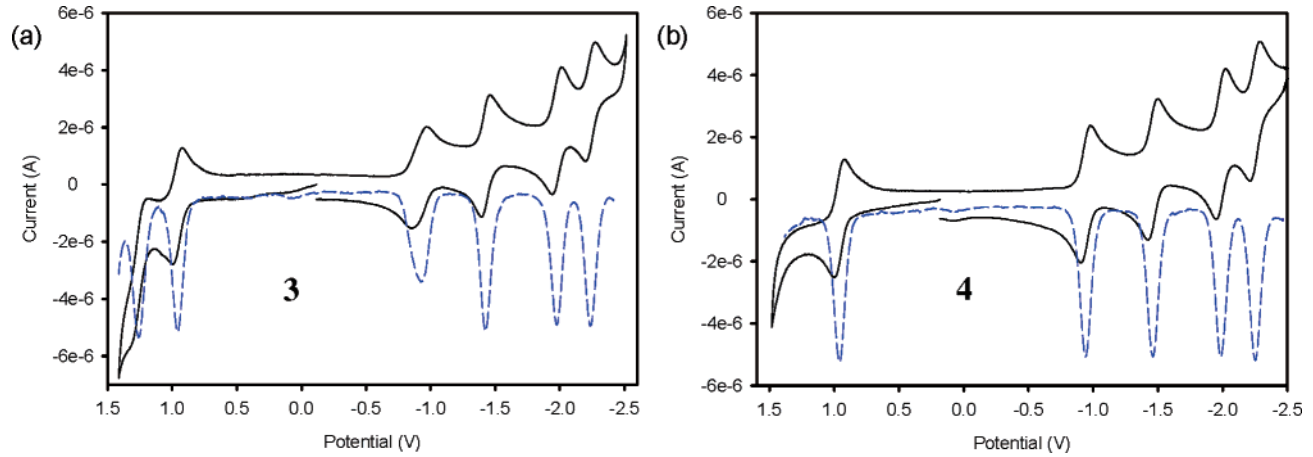

Figure 3. Cyclic (−) and square (blue - - -) wave voltammograms of (a) **3** and (b) **4** in acetonitrile vs the ferrocinium/ferrocene-couple using a Ag/Ag^+ reference electrode with 0.1 M Bu_4NPF_6 as supporting electrolyte.

The cyclic and square wave voltammograms of the Ru(II) complexes **3** and **4** are presented in Figure 3. In the voltammogram of **4**, two reversible one-electron reduction processes for coordinated **2** (−0.95, −1.47 V) and subsequently two reversible bpy-based one-electron reductions (−1.99 and −2.26 V) are observed. These concur with the assignments made for **3** where two stepwise reduction processes occur on the coordinated N-HSB **1** before those on the bpy.[2] Coordination to the Ru^{II} center facilitates the reduction processess of **1** and **2** almost equally (approximately 0.6 V anodic shift in each case).

In contrast to **3**, which has two reversible one-electron oxidation processes at anodic potential, **4** has only one observable oxidation process. The reversible oxidation wave of **4** and the first reversible oxidation wave of **3** (both at +0.95 V) fall within the potential range typical of Ru-based oxidations.[14] X-band EPR analyses of these electrochemically generated, single oxidized complexes $[Ru(bpy)_2(\mathbf{1})]^{3+}$ and $[Ru(bpy)_2(\mathbf{2})]^{3+}$ as frozen CH_3CN solutions give rise to well-resolved rhombic spectra with large g tensor anisotropy (one-electron oxidized **3**, $g_x = 2.900$, $g_y = 2.500$, $g_z = 2.300$; one-electron oxidized **4**, $g_x = 2.850$, $g_y = 2.500$, $g_z = 2.300$). They are consistent with low-spin $4d^5$ configurations.[15] The second wave at +1.26 V in the cyclic voltammogram of **3** is assigned to an oxidation process of complexed ligand **1**. The absence of this wave in **4** suggests a correlation with it and the more extended π-system of **1**. The wave appears distorted because it is located close to the border of the accessible potential range; however, the reverse peak is clearly visible in the SQW. Coordination to the Ru^{III} center shifts the ligand oxidation potential by approximately 0.4 V (see Table 1). This is surprisingly small as compared to the anodic shift in the ligand reduction processes and suggests that the oxidation site is remote from the Ru center.

No evidence for the dimeric aggregation proposed for **3**[2] is evident in either the cyclic and square wave voltammograms or the NMR spectroscopic studies of **4**. The same cannot be said for **3**, where further evidence for the persistence of dimeric aggregates in solution can be gleaned from the broadening of the first reduction wave of this complex in both its cyclic and square wave voltammograms. A similar phenomenon has been observed for $[Ru(bpy)_2(eilatin)]^{2+}$, where, on increasing concentration, the reduction process ultimately becomes split into two separate waves, each of half the current density of subsequent ones.[4]

Spectroelectrochemistry. To get an impression of the stability of the various oxidation states of the complexes, sample volumes of solutions of **3** and **4** were reduced and oxidized by bulk electrolysis at appropriate fixed potentials (controlled potential coulometry, CPC; at −25 °C). The

(13) For the purpose of this work, a redox process is considered reversible when the two peak currents for each redox couple have the same height at different scan rates (0.05−0.5 V s^{-1}), and the peak separations (at lower scan rates) are close to those observed for the reversible ferrocene couple under the same conditions (0.06−0.08 V).

(14) (a) Balzani, V.; Juris, A.; Venturi, M.; Campagna, S.; Serroni, S. *Chem. Rev.* **1996**, *96*, 759−833. (b) Juris, A.; Balzani, V.; Barigelletti, F.; Campagna, S.; Belser, P.; von Zelewsky, A. *Coord. Chem. Rev.* **1988**, *84*, 85−277.

(15) (a) Morris, D. E.; Hanck, K. W.; DeArmond, M. K. *J. Am. Chem. Soc.* **1983**, *105*, 3032−3038. (b) Kaim, W.; Ernst, S.; Kasack, V. *J. Am. Chem. Soc.* **1990**, *112*, 173−178. (c) Lahiri, G. K.; Bhattacharya, S.; Ghosh, B. K.; Chakravorty, A. *Inorg. Chem.* **1987**, *26*, 4324−4331. (d) Ghosh, P.; Pramanik, A.; Bag, N.; Lahiri, G. K.; Chakravorty, A. *J. Organomet. Chem.* **1993**, *454*, 237−241.

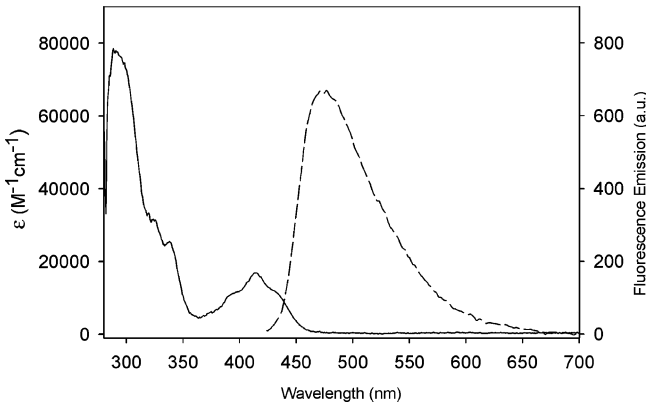

Figure 4. The absorption (−) and emission (---) (after excitation at λ = 415 nm) spectra of **2** in toluene.

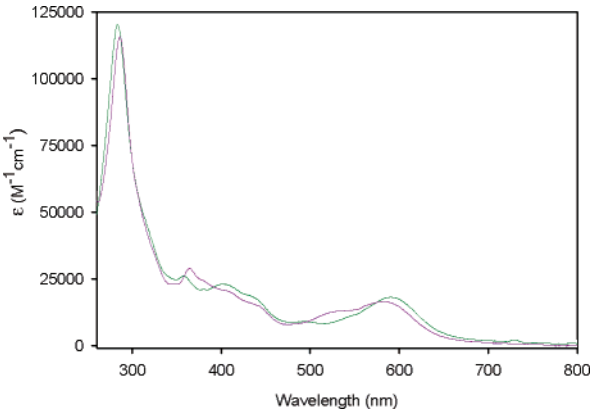

Figure 5. The absorption spectrum of **4** in acetonitrile (green −) and chloroform (purple −) solution.

Figure 6. (a) Chloroform and (b) acetonitrile solution of **4**.

progress of the respective oxidation or reduction process was monitored through UV−vis spectral changes recorded in situ during coulometry. It was found that for all processes the current dropped to background levels when a charge corresponding to one-electron per mole had passed; that is, the waves of the voltammograms arise from one-electron redox processes.

With **3**, it was found that the $[Ru(bpy)_2(\mathbf{1})]^-$, $[Ru(bpy)_2(\mathbf{1})]^0$, $[Ru(bpy)_2(\mathbf{1})]^+$, $[Ru(bpy)_2(\mathbf{1})]^{2+}$, and $[Ru(bpy)_2(\mathbf{1})]^{3+}$ forms are stable over at least 40 min at −25 °C. There was no evidence for decomposition of any oxidized or reduced species in the UV−vis spectra, and the SQW voltammograms after each oxidation and reduction were identical to those of the starting material. The dimeric aggregation of $[Ru(bpy)_2(\mathbf{1})]^{2+}$ is evident from both NMR and SQW studies. During coulometry, the $[Ru(bpy)_2(\mathbf{1})]^{2+}$ to $[Ru(bpy)_2(\mathbf{1})]^+$ bulk reduction (at −25 °C) was found to proceed slowly. We believe this is because the dimerized starting material monomerizes prior to further reduction. As with other ruthenium dimer complexes,[4] the $[Ru(bpy)_2(\mathbf{1})]^{2+}$ to $[Ru(bpy)_2(\mathbf{1})]^{3+}$ oxidation does not exhibit a broad voltammetric peak or slow electrolysis.

With **4**, it was found that the $[Ru(bpy)_2(\mathbf{2})]^0$, $[Ru(bpy)_2(\mathbf{2})]^+$, $[Ru(bpy)_2(\mathbf{2})]^{2+}$, and $[Ru(bpy)_2(\mathbf{2})]^{3+}$ forms had stability similar to those of **3**, but $[Ru(bpy)_2(\mathbf{2})]^-$ undergoes slow decomposition with the appearance of two extra peaks in the SQW voltammogram. As the height and position of the two peaks associated with the reduction of bpy were maintained during decomposition, it would appear that it is the doubly reduced coordinated **2** that is unstable.

Photophysical Properties. The UV−vis and fluorescence spectra of **2** in toluene solution are presented in Figure 4. The electronic absorption spectrum of nonplanar **2** is markedly similar to that of the parent N-HSB **1** in terms of overall shape.[1] However, it lacks the clear fine structure for which the rigidity, planarity, and aggregation of **1** were responsible.[16] The λ_{max}^{abs} in the UV−vis spectrum of **2** (291 nm, ϵ_{max} = 78 000, toluene) appears at higher energy than that of **1** (355 nm, ϵ_{max} = 140 000, toluene) with a significant reduction in ϵ_{max}. Similarly, the lowest energy band of **2** (429 nm) is blue-shifted with respect to **1** (481 nm). These findings are in agreement with the reduction of conjugation and the depletion of π-electron density in **2**. A shift of the emission maximum in toluene from green in N-HSB **1** (λ_{em} = 494 nm, ϕ_F = 0.40) to blue in N-$^1/_2$HSB **2** (λ_{em} = 474 nm, ϕ_F = 0.55) is a further consequence of the diminution in π/π^* framework. The arrival of **2** is a step toward a new generation of intensely fluorescing nitrogen-heterosuperbenzenes emitting at a variety of wavelengths. With most well-developed organic polymer and conjugated molecular systems being red to green light emitting materials,[17] **2** is an important member of the more limited group of compounds that emit in the blue region.

The UV−vis spectrum of **4** (Figure 5) is similar to that reported for other polypyridyl ruthenium complexes.[14b] In the acetonitrile spectrum, there are two bands at 284 and 358 nm due to ligand-centered (LC) $\pi-\pi^*$ transitions on coordinated bpy and N-$^1/_2$HSB, respectively, and in the visible region two superimposed bands at around 400−450 nm, which are assigned to the ^{1}MLCT of coordinated bpy and a low-energy LC $\pi-\pi^*$ of coordinated **2**. At lower-energy still (591 nm) is the red-shifted ^{1}MLCT absorption due to the N-$^1/_2$HSB. The low-lying π^* acceptor orbitals on **2** are responsible for the excessively low-energy of this transition. The overall consequence of these absorptions is that the heteroleptic **4** has appreciable and more uniform

(16) (a) Fleming, A.; Coleman, J. N.; Dalton, A. B.; Fechtenkötter, A.; Watson, M. D.; Müllen, K.; Byrne, H. J.; Blau, W. J. *J. Phys. Chem. B* **2003**, *107*, 37−43. (b) Ogliaruso, M. A.; Becker, E. I. *J. Org. Chem.* **1965**, *30*, 3354−3360. (c) Nijegorodov, N. I.; Downey, W. S. *J. Phys. Chem.* **1994**, *98*, 5639−5643.

(17) (a) Kraft, A.; Grimsdale, A. C.; Holmes, A. B. *Angew. Chem., Int. Ed.* **1998**, *37*, 402−428. (b) Rees, I. D.; Robinson, K. L.; Holmes, A. B.; Towns, C. R.; O'Dell, R. *Mater. Res. Bull.* **2002**, *27*, 451−455.

Table 2. Spectroscopic Properties of the Near-Infrared Emitter **4** in Various Solvents Together with Those of **3** and $[Ru(bpy)_3]^{2+}$ at Room Temperature

complex	solvent	wavelength of lowest energy absorption band (nm) (ϵ (M^{-1} cm^{-1}))	wavelength of highest energy emission band (nm)	τ (ns)	ϕ_F
3[a]	$CHCl_3$	620 (8×10^3)	840	39	7×10^{-4}
3[a]	CH_3CN	615 (15×10^3)	880	13	4×10^{-4}
3[a]	butyronitrile[c]		800[c]		
4	$CHCl_3$	581 (17×10^3)	840	23	7×10^{-4}
4	CH_3OH	583 (16×10^3)	851	9	2×10^{-4}
4	CH_3CN	591 (18×10^3)	868	11	3×10^{-4}
4	butyronitrile[c]		798[c]		
$[Ru(bpy)_3]^{2+}$ [b]	CH_3CN	452 (13×10^3)	615	800	6.2×10^{-2}

[a] Reference 2. [b] Reference 18. [c] 77 K.

absorption throughout the visible region than its N-HSB analogue **3**. It is undoubtedly deserving of the title "black" absorber.[3]

The low-energy LC and ^{1}MLCT absorption bands of **4** show solvent dependence. The impact of these on the color of the Ru(II) complex in chloroform solution and acetonitrile solution is dramatic (see Figure 6).

Large-surface aromatic ligands, offering extended π/π^* frameworks, are known to lower the energy of the acceptor level in heteroleptic Ru(II) polypyridyl complexes and stabilize the excited electron.[3a] The resulting reduction in the excited-to-ground-state energy gap can shift the emission into the near-IR. The extended π-system of N-$^1/_2$HSB, although considerably reduced as compared to its "parent", is still sufficient to ensure that **4** is a near-IR emitter (λ_{em} = 868 nm, acetonitrile). There is a small decrease in the excited-state lifetime and quantum efficiency of this emission as compared to that of **3** (see Table 2). This is to be expected on consideration of the lower rigidity of the N-$^1/_2$HSB framework flanked by two "uncyclized" phenyl rings. Rigidity is known to assist in reducing nonradiative decay and to help prolong excited-state lifetimes.[3e] The emission spectra of **4** at room temperature and at 77 K are presented in Figure 7. In low-temperature rigid glasses, the emission is clearly blue-shifted to λ_{em} = 798 nm and begins to display vibrational structure.[19]

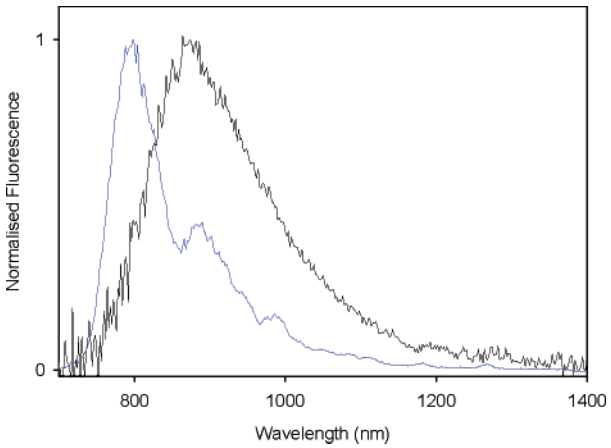

Figure 7. The corrected emission spectra of **4** at room temperature (−) (after excitation at λ = 627 nm) and at 77 K (blue −) (after excitation at λ = 591 nm).

Conclusion

Modification, as reported here, of the key oxidative cyclodehydrogenation step in the formation of heteropolyaromatics is a promising synthetic achievement. The arrival of the "half-cyclized" daughter N-$^1/_2$HSB **2** proclaims a notable extension to the nitrogen-heterosuperbenzene family. The unusual optical and electronic properties of the founding N-HSB **1** persist in N-$^1/_2$HSB **2** despite the considerable reduction in aromaticity from 13 to 8 fused ring systems. Uniquely **2** offers a nonaggregating platform flanked by two "uncyclized" and nonplanar phenyl rings and marks a first step in the systematic study of the molecular and supramolecular properties of this rare type of molecule. By virtue of its locked pyrimidine N atoms, **2** is gifted with the opportunity for bidentate ligand functionality. It is a valuable comparator for the few known acceptor ligands with the exceptionally low lying π^* orbitals necessary to red-shift the MLCT transition(s) of heteroleptic Ru(II) polypyridyl complexes. Its complex $[Ru(bpy)_2(\mathbf{2})]^{2+}$ **4** is another addition to the group of compounds known as "black" absorbers and near-IR emitters and represents an advance in the design of chemically accessible and tunable photoactive materials.

Acknowledgment. We thank Dr. Eckhard Bill, Prof. Karl Wieghardt, Dr. Roberto Ballardini, and Prof. Maria Teresa Gandolfi for useful discussions, and Dr. John O'Brien for technical assistance. D.J.G. thanks Enterprise Ireland award IF-2001\369 for financial support.

Supporting Information Available: ESI-MS of **2** and ESI-MS and ^{1}H NMR spectra of **4**. The ^{1}H−^{1}H TOCSY NMR spectrum of **4**. The cyclic voltammograms of **1** and **2**. EPR spectra of **3** and **4**. This material is available free of charge via the Internet at http://pubs.acs.org.

IC050335N

(18) Barigelletti, F.; De Cola, L.; Balzani, V.; Belser, P.; von Zelewsky, A.; Vögtle, F.; Ebmeyer, F.; Grammenudi, S. *J. Am. Chem. Soc.* **1989**, *111*, 4662−4668.
(19) Di Donato, E.; Tommasini, M.; Fustella, G.; Brambilla, L.; Castiglioni, C.; Zerbi, G.; Simpson, C. D.; Müllen, K.; Negri, F. *Chem. Phys.* **2004**, *301*, 81−93.